REPORT DOCUMENTATION PAGE

Form Approved OMB No. 0704-0188

1. AGENCY USE ONLY *(Leave blank)*

2. REPORT DATE
31 May 1996

3. REPORT TYPE AND DATES COVERED
Summary 01 June 95 - 31 May 96

4. TITLE AND SUBTITLE
Fundamental Studies of Radial Wave Thermoacoustic Engines

5. FUNDING NUMBERS
PE 61153N
G N0001493 J 1131

6. AUTHOR(S)
W. Patrick Arnott

7. PERFORMING ORGANIZATION NAME(S) AND ADDRESS(ES)
Atmospheric Sciences Center
Desert Research Institute
P.O. Box 60220
Reno NV 89506-0220

8. PERFORMING ORGANIZATION REPORT NUMBER

9. SPONSORING/MONITORING AGENCY NAME(S) AND ADDRESS(ES)
Office of Naval Research
ONR 331
800 North Quincy Street
Arlington VA 22217-5660

10. SPONSORING/MONITORING AGENCY REPORT NUMBER

11. SUPPLEMENTARY NOTES

12a. DISTRIBUTION / AVAILABILITY STATEMENT
Approved for public release:
Distribution unlimited

19960621 104

13. ABSTRACT *(Maximum 200 words)*

The influence of resonator and stack geometry on thermoacoustic refrigerator performance is investigated. The current focus is on the radial mode of a cylindrical resonator and parallel plate stacks. Progress in the past year has been development of a numerical model to evaluate and optimize radial refrigerator performance, and contribution of a hot end heat exchanger to the radial wave prime mover now operating at the University of Mississippi. The numerical model was used to evaluate a plane-wave heat-driven thermoacoustic sound source driving a radial-wave refrigerator. Optimization improved the overall efficiency of the intuitive design by an order of magnitude. The refrigerator was predicted to operate at 25% of the Carnot coefficient of performance, and the prime mover at 28% of the Carnot efficiency. The optimization results were explored to evaluate implications of design features including relative stack placement in the standing wave, stack plate spacing relative to the thermal penetration depth, the trade-offs between kinetic and potential energy dissipation and thermoacoustic power generation, and the dynamical stack temperature distribution relative to the static result that depends only on stack and gas thermal conductivity.

14. SUBJECT TERMS
Thermoacoustic, refrigeration, Heat-Driven Sound Source, Radial Geometry

15. NUMBER OF PAGES
27

16. PRICE CODE

17. SECURITY CLASSIFICATION OF REPORT	18. SECURITY CLASSIFICATION OF THIS PAGE	19. SECURITY CLASSIFICATION OF ABSTRACT	20. LIMITATION OF ABSTRACT
UNCLASSIFIED	UNCLASSIFIED	UNCLASSIFIED	

Annual Summary Report
FUNDAMENTAL STUDIES OF RADIAL WAVE THERMOACOUSTIC ENGINES

June 1996

by
W. Patrick Arnott
Atmospheric Sciences Center
Desert Research Institute
PO Box 60220
Reno NV 89506

for
Office of Naval Research
Dr. Logan E. Hargrove

ABSTRACT

The influence of resonator and stack geometry on thermoacoustic refrigerator performance is investigated. The current focus is on the radial mode of a cylindrical resonator and parallel plate stacks. Progress in the past year has been development of a numerical model to evaluate and optimize radial refrigerator performance, and contribution of a hot end heat exchanger to the radial wave prime mover now operating at the University of Mississippi. The numerical model was used to evaluate a plane-wave heat-driven thermoacoustic sound source driving a radial-wave refrigerator. Optimization improved the overall efficiency of the intuitive design by an order of magnitude. The refrigerator was predicted to operate at 25% of the Carnot coefficient of performance, and the prime mover at 28% of the Carnot efficiency. The optimization results were explored to evaluate implications of design features including relative stack placement in the standing wave, stack plate spacing relative to the thermal penetration depth, the trade-offs between kinetic and potential energy dissipation and thermoacoustic power generation, and the dynamical stack temperature distribution relative to the static result that depends only on stack and gas thermal conductivity.

Annual Summary Report
FUNDAMENTAL STUDIES OF RADIAL WAVE THERMOACOUSTIC ENGINES

TABLE OF CONTENTS

1. Project Description

The goal of our research (in close collaboration with Richard Raspet and students from the Univ. MS) is to determine the merits of alternative geometry thermoacoustic refrigerators. Our primary emphasis has been on the radial mode of cylindrical resonators though the eventual formalism is general.

2. Approach taken.

A linear theoretical model was derived for predicting the first order acoustic and second order heat and work flow quantities for thermoacoustic heat engines. The model was based on Swift's results[1] for this geometry, though we added generality to simplify numerical analysis.[2] The short stack analytical approximation was derived to compare engine performance in plane and radial wave resonators. The numerical model developed was previously only useful for predicting the onset temperature, quality factor, and resonant frequency of prime movers, though has now been extended to predict the full performance of prime movers and refrigerators. The numerical model is similar in rigor to the model DELTAE (Design Environment for Linear Thermoacoustic Engines) developed at Los Alamos National Laboratory by Bill Ward and Greg Swift, though differs in the inclusion of the radial geometry and variable stack plate spacing. A key component of the model is a subroutine to stretch and shrink the physical lengths and plate spacings of the thermoacoustic elements to find designs that optimize the overall efficiency. Experience in both design and construction of thermoacoustic engines has indicated that models predict an upper limit for system performance, are useful for considering many potential designs before the timely and costly process of construction begins, and can enhance intuition about system performance when the model output is fully explored.

3. Specific work accomplished, June 1995 - May 1996.

Accomplishments are given in separate theory and experiment sections below. A brief summary will be given to introduce these sections. A numerical model was

developed to evaluate radial wave refrigerators and prime movers. This model is similar in rigor to the Los Alamos model, DELTAE. The primary application was to evaluate a radial refrigerator driven by a plane wave prime mover. Boundary conditions were developed to connect the plane wave and radial wave resonators. An optimization routine was developed to assist in evaluation of many system configurations. This routine took an intuitively-designed heat-driven refrigerator and significantly improved the performance of the prime mover and refrigerator. The system designed by the routine was thoroughly evaluated as a reality check of the routine and as a means to improve on intuition for thermoacoustics. One particularly interesting result of the optimization routine was the prediction that the prime mover stack plate spacing should be narrower than the short stack approximation would suggest, because the dynamical temperature gradient that generates sound is considerably increased by narrowing the plate spacing. This result was for a relatively low thermal conductivity stack (compared with a stainless steel stack) that had the temperature distribution strongly influenced by the acoustic wave and less influenced by stack thermal conductivity.

The radial wave prime mover at the University of Mississippi finally has gone into oscillation after considerable effort by Jay Lightfoot! We designed and built a hot end heat exchanger at DRI for the prime mover. Work is currently underway to compare prime mover performance predictions with measurements.

3a. Theory A radial wave refrigerator driven by a plane wave prime mover was evaluated with the numerical model developed during the past year. The purpose was to continue to develop understanding of acoustic refrigerator performance in alternative geometry resonators (other than the usual plane wave resonator), and to evaluate a heat driven refrigerator that does not compromise either the prime mover or refrigerator performance by requiring them to be adjacent as in the original Wheatley beer cooler.[1] The program was designed to produce numbers for efficiency and cooling capacity as well as details of the system such as the pressure and volume velocity throughout the

system. These details are essential for improving the intuitive model of thermoacoustics that is based on the analytical short stack approximation. To run the program, one edits a file that contains a starting system with choices for stack plate spacing and location in the resonator, heat exchanger properties, ambient gas pressure, heat input at the prime mover and heat load at the refrigerator, and overall system dimensions such as resonator cross sectional area. The starting system design is usually obtained from either the short stack approximation, or trial and error. Only a summary of the program, the beer cooler design, and the most interesting implications will be given here.

Figure 1 schematics the heat driven acoustic refrigerator. A plane wave thermoacoustic prime mover driven by an unspecified heat source is the acoustic source to drive the radial wave acoustic refrigerator. The schematic is roughly correct in the relative size of the resonator segments and the stack locations determined from the optimization program. The locations of pressure nodes are shown for reference. The relevant theory for each section of the system is given in summary form below. Boundary conditions applied at the radial resonator and cone interface were that acoustic pressure in the radial resonator at the cone radius r_c was taken the same as the acoustic pressure at the narrow end of the cone, and volume velocity was made continuous by considering the net volume flow into a differential element of radius r, thickness dr, and height H. Design criteria of the heat driven refrig are given below, followed by a table indicating the predicted performance.

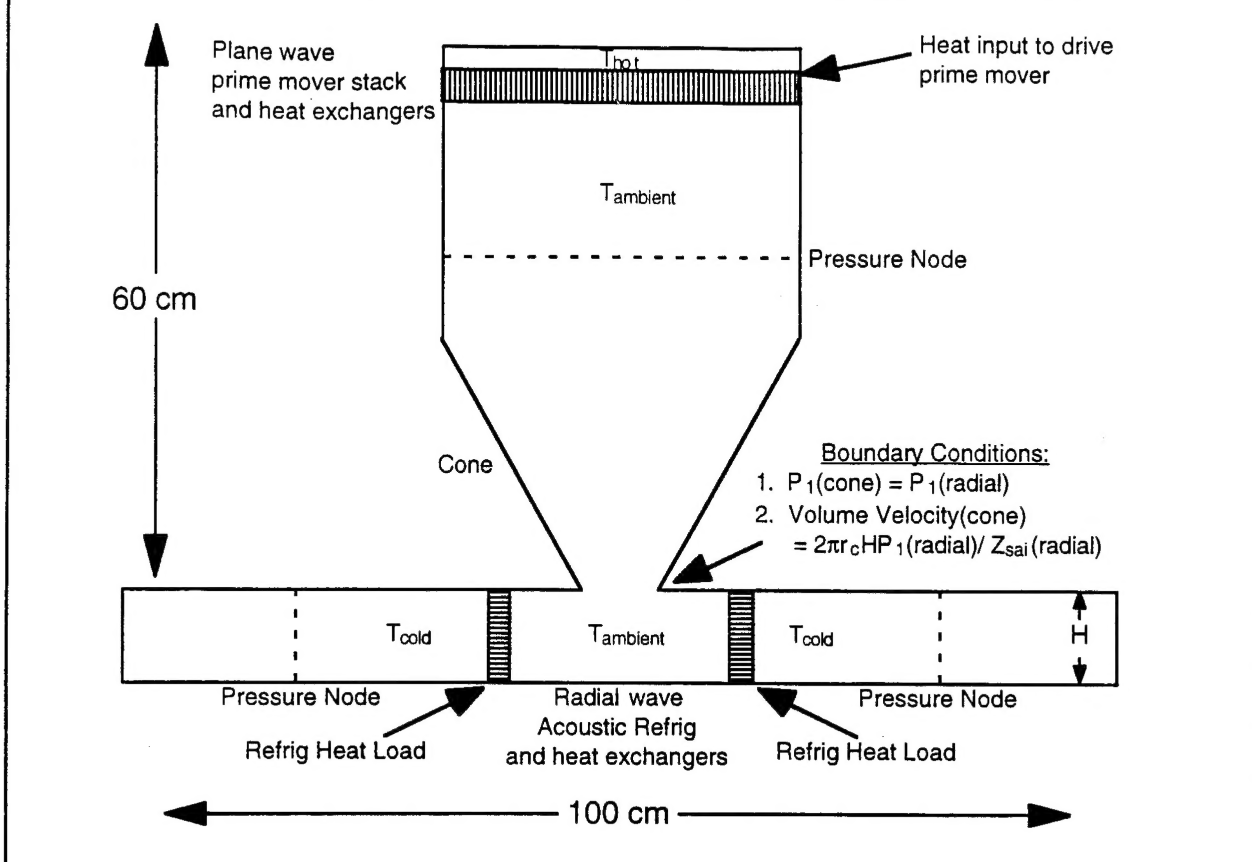

Figure 1. Plane wave prime mover for the radial wave refrigerator.

Radial Wave Refrigerator

(Rott's Equations, modified by Swift[1] for Radial Waves, as outlined by Arnott, et. al., Ref. 2).

Heat Exchangers and Resonator Sections

Counter propagating cylindrical traveling waves superimposed to meet pressure and impedance continuity at boundaries.

Refrigerator Stack

Numerical integration of three coupled 1st order Differential Equations:
Acoustic pressure   Volume velocity   Stack ambient temperature

Transition Element From Radial to Plane: The Cone

(Webster's Horn Equation with dissipation included).
Numerical integration of two coupled 1st order Differential Equations:
Acoustic pressure   Volume velocity.

Plane Wave Prime Mover

(Rott's Equations as outlined in Arnott, et. al., Ref. 3).

Heat Exchangers and Straight Resonator Sections

Counter propagating plane traveling waves superimposed to meet pressure and impedance continuity at boundaries.

Prime Mover Stack

Numerical integration of three coupled 1st order Differential Equations:
Acoustic pressure   Volume velocity   Stack ambient temperature

DESIGN CRITERIA:	
FLUID: MOLAR MIXTURE 60%He 40%Ar	N_{PR} = 0.392 $P_{ambient}$ = 300 kPa.
COOLING CAPACITY **100 WATTS**	2.2 LITERS OF WATER / HOUR TO COLD TEMPERATURE FROM ROOM
COLD END TEMPERATURE	255 K = -18 C
AMBIENT TEMPERATURE 22 C	**REFRIG TEMPERATURE SPAN=40 C**
HOT END TEMPERATURE ≈ 327 C	**PRIME MOVER SPAN ≈ 305 C**

Table 1. Predicted parameters of the heat driven acoustic refrigerator.

RESULTS OF INTUITIVE DESIGN		RESULTS OF OPTIMIZATION	
Frequency	677 Hz	Frequency	535 Hz
Acoustic Pressure / Ambient Pressure	0.95%	Acoustic Pressure / Ambient Pressure	1.7%
Heat Input	5001 WATTS	Heat Input	495 WATTS
Hot End Temperature	316 K	Hot End Temperature	330 K
Prime Mover Actual Efficiency / Carnot Efficiency	5.4% / 50.0% = 10.9%	**Prime Mover** Actual Efficiency / Carnot Efficiency	14.3% / 51.1% = 28.1%
Refrigerator Actual COP / Carnot COP	0.38 / 6.38 = 6.0%	**Refrigerator** Actual COP / Carnot COP	1.56 / 6.38 = 24.5%
Overall Cooling Capacity / Heat Input	2.0%	**Overall** Cooling Capacity / Heat Input	20.2%
Actual Overall / Carnot Overall	0.63%	Actual Overall / Carnot Overall	6.2%

The predicted performance in Table 1 is separated into 2 columns. The column on the left is the performance of the beer cooler designed by intuition, and the column on the right is performance after optimization. Optimization was performed by stretching and shrinking the elements listed below to see if a system with higher overall efficiency could be obtained. The optimization was loosely constrained to prevent the prime mover hot end temperature from increasing without bound. Constrainment was achieved by actually optimizing the product of overall efficiency and penalty where penalty progressively decreased below unity if the newly computed hot end temperature strayed from the requested value T_{hot} = 316 K. A progressive penalty was essential because the optimization algorithm had 'room' to work, but ensured a reasonable hot end temperature.

Quantities Adjusted to Optimize the Overall Efficiency

Prime mover stack length
Resonator length at the hot end
Resonator length between the ambient end of the prime mover and the cone
Prime mover and its heat exchangers plate spacings
Refrigerator and its heat exchangers plate spacings
Refrigerator stack length
Radial resonator length from the wall to the cold heat exchanger
Radial resonator length from the center to the ambient heat exchanger
Length of the cone

Table 1 clearly indicates the utility of optimization. The bottom line overall efficiency was improved by an order of magnitude by applying optimization. Other quantities can and have been added to the list of values adjusted in seeking optimization, though this work is in a preliminary stage at the moment. The refrigerator COP was computed as 25% of the Carnot COP, and is likely an upper limit to the actual COP one would achieve in a real device. It perhaps is possible to improve the COP by optimizing this quantity alone. Heat exchangers were included in the design, though were not as carefully designed for handling their heat loads as would be necessary in preparation for device construction. In other words, the heat exchangers were shorter than they would be in a practical device. The quantity of heat needed to power the prime mover does not preclude the use of solar energy.

The intuitive design clearly was far from useful as indicated by the comparison of the two columns in Table 1. Implications of the optimization code are presented in the remainder of this section as a reality check and perhaps as a guide for updating intuition. Figure 2 shows the system configuration that will be used to understand where the various parts of the heat driven refrigerator are located with respect to the acoustic quantities to be considered. Positive coordinate values are values of radius for the radial resonator in Fig. 1, and negative values are the plane wave resonator. Numerical analysis begins in the radial resonator at the rigid wall, and completes at the hot end of the prime mover. The program adjusts the starting acoustic pressure amplitude, frequency, and heat input to the prime mover until the boundary conditions of ambient end refrigerator temperature and complex specific acoustic impedance at the rigid termination of the prime mover are met.

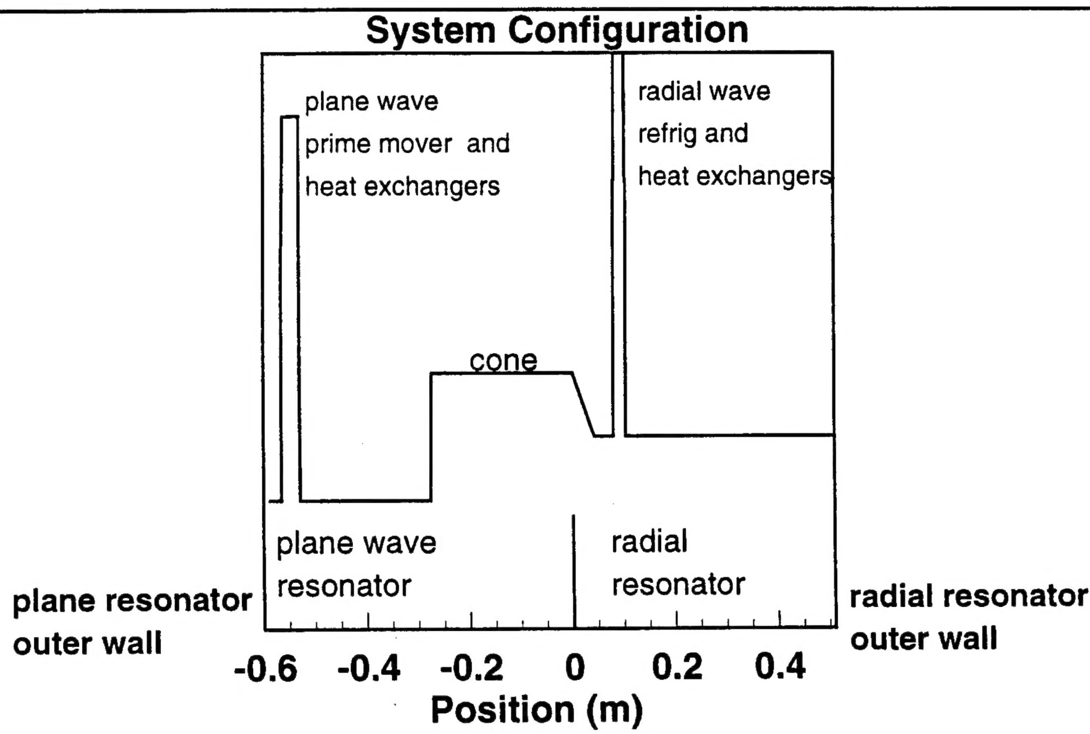

Figure 2. Location of thermoacoustic elements relative to the position coordinate.

Figure 3 shows the modal acoustic pressure with an overlay of the system configuration shown in Fig. 2. Note that the acoustic pressure in the cone is analogous to the radial resonator profile near the center as one would expect. Note also that the stacks are in regions of relatively high pressure.

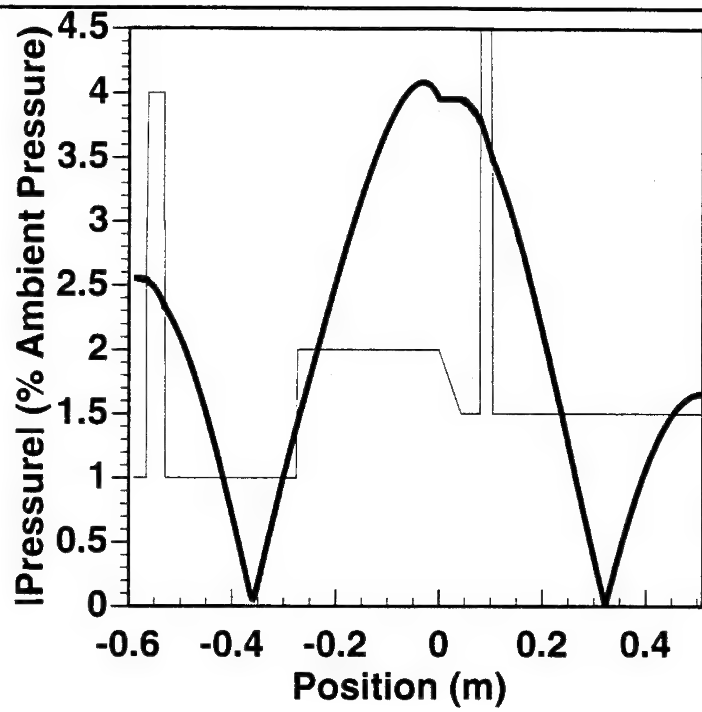

Figure 3. Acoustic pressure.

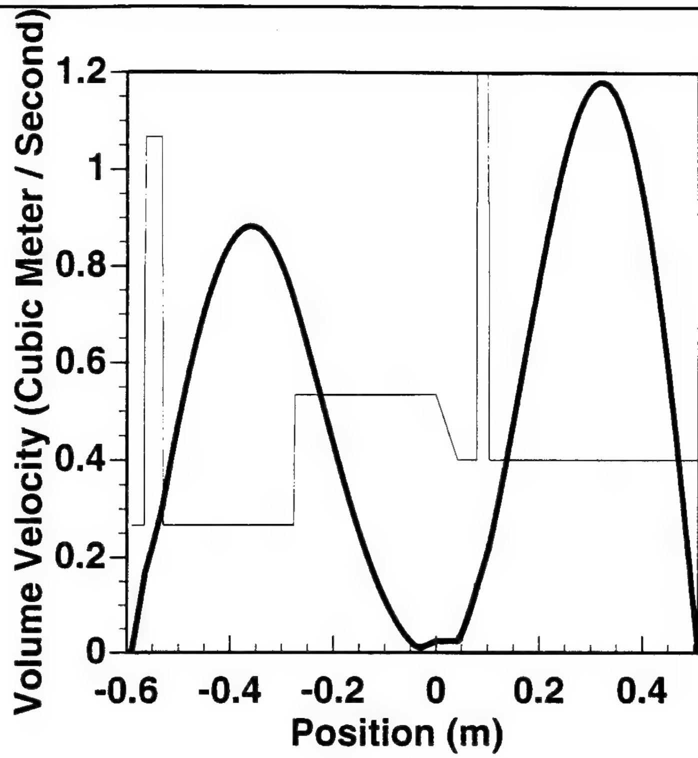

Figure 4. Volume Velocity.

Figure 4 shows the volume velocity distribution. More than 1 cubic meter of gas oscillates per second through a radius of 0.3 m in the radial resonator. Stacks are at comparible volume velocities. The volume velocity is lowest at the transition from radial resonator to cone, purposely, to mode match the radial and plane wave resonators.

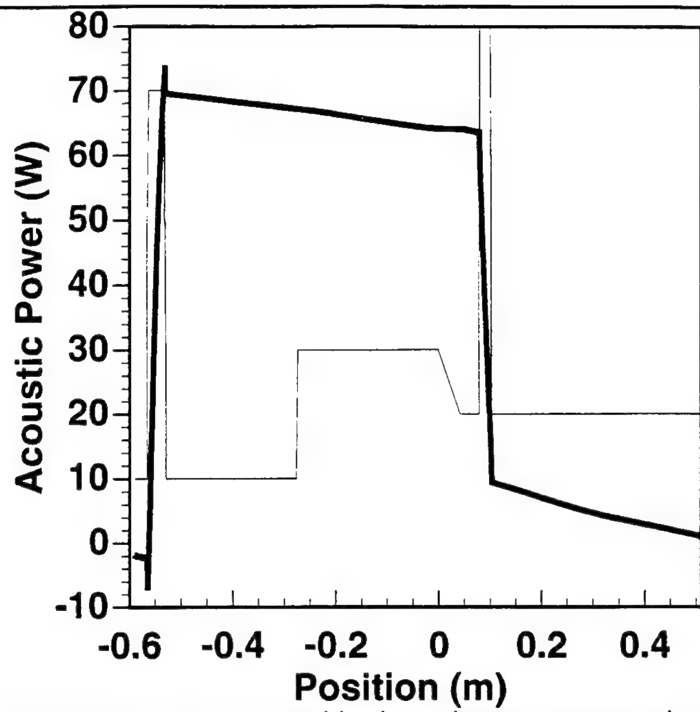

Figure 5. Acoustic power generated in the prime mover stack and dissipated elsewhere.

Figure 5 shows the generation of acoustic power in the prime mover stack and its dissipation elsewhere. Negative values indicate the direction of power flow. The spikes near -0.6 m near the prime mover are due to large power dissipation in the heat exchangers. Power flows out of the prime mover to the refrigerator where it stimulates heat transport, and flows to the rigid termination at the far right where thermal dissipation consumes a few Watts.

Figure 6 shows the stored kinetic, potential, and 'thermoacoustic' energy in the resonator. Note specifically that KE and PE are not the dissipated amounts, but are only proportional to these quantities. Peak KE dissipation is generally larger than PE dissipation by approximately a factor of 2. Trading off some thermoacoustic power by moving the stacks away from peaks of this quantity (lower panel) results in a savings of KE dissipation due to gas viscosity (upper panel).

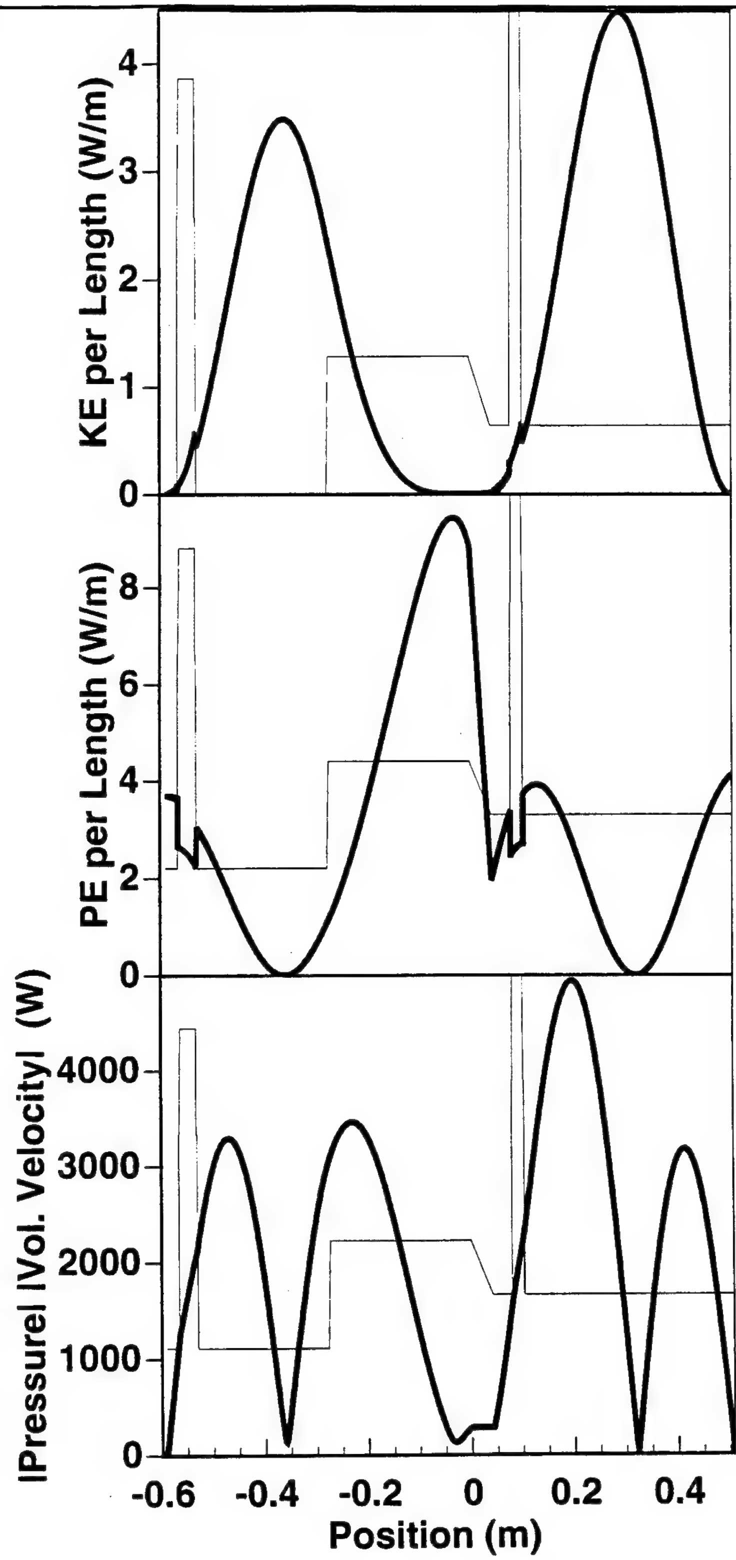

Figure 6. Kinetic, potential, and thermoacoustic power distributions.

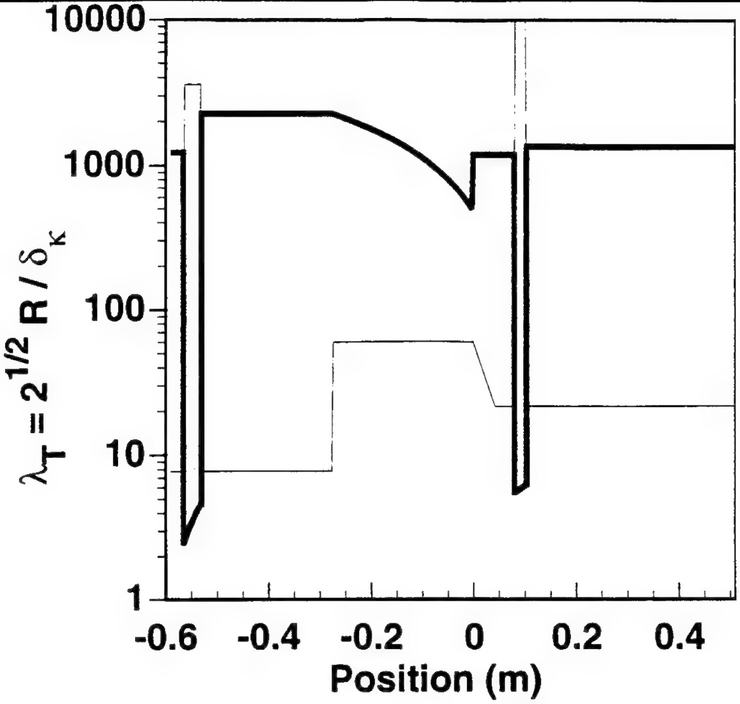

Figure 7. Ratio of characteristic dimension and thermal boundary layer thickness.

Figure 7 shows the normalized characteristic dimension of the thermoacoustic elements. This dimension is simply the stack and heat exchanger plate spacings, or local resonator radius, divided by the local thermal boundary layer thickness. Note that the stack plate spacing determined by the optimization routine is greater for the radial wave refrig than for the plane wave prime mover. This is qualitatively consistent with the short-stack, optimized refrigerator intercomparison presented in Ref. 2. Details of stack plate spacings will be considered more thoroughly below.

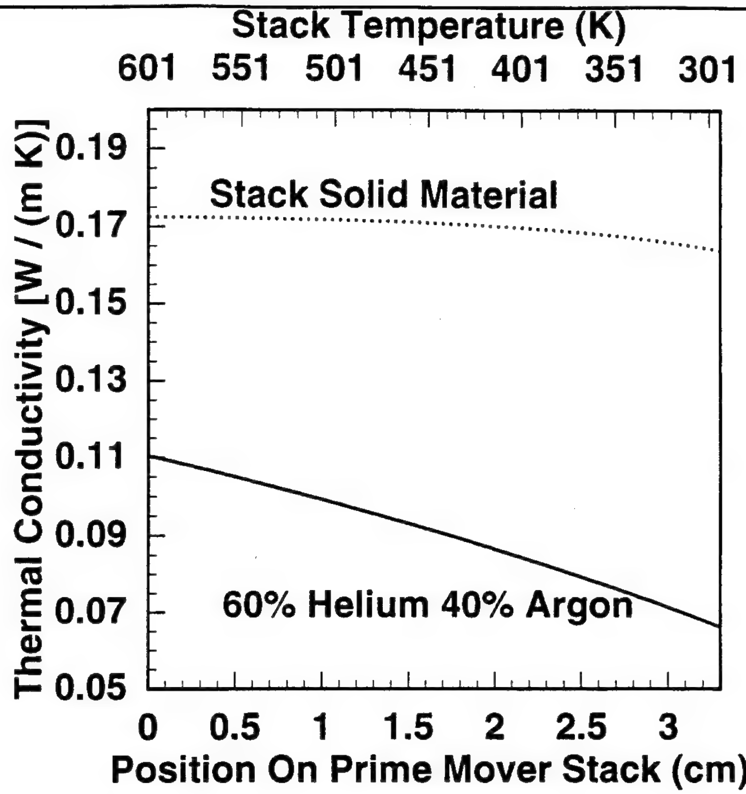

Figure 8. Prime mover stack solid and gas thermal conductivities.

The next four figures are a detailed interpretation of the prime mover stack properties. To start off, Fig. 8 shows the thermal conductivity of the stack solid material and of the gas. Position in the stack is given by the lower axis, and temperature by the upper horizontal axis. The temperature dependence of the stack solid material thermal conductivity was determined by using the room temperature value of silicone bonded mica paper with the temperature dependence of Kapton (we have not been able to find the temperature dependence of thermal conductivity for mica paper). The use of Swift's non-ideal thermal solid parameter[1] ε_s is necessary for the gas/solid combination considered because their thermal conductivities are comparable.

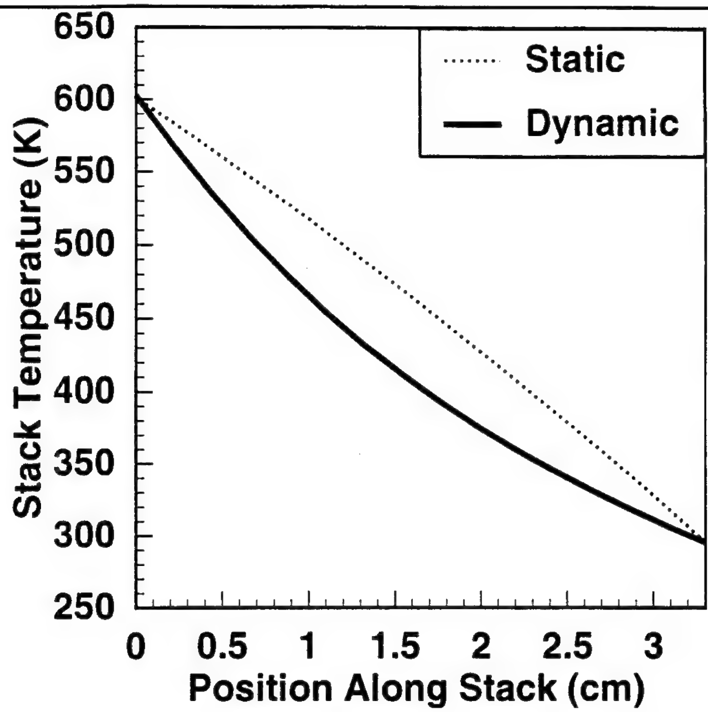

Figure 9. Prime mover static and dynamic temperature distributions.

Figure 9 shows the static and dynamic temperature distributions in the prime mover stack. The static distribution occurs when no acoustic wave is present. The acoustic wave adds 2 extra path ways for heat transfer in the stack, in addition to thermal conductivity, as discussed in Ref. 2.

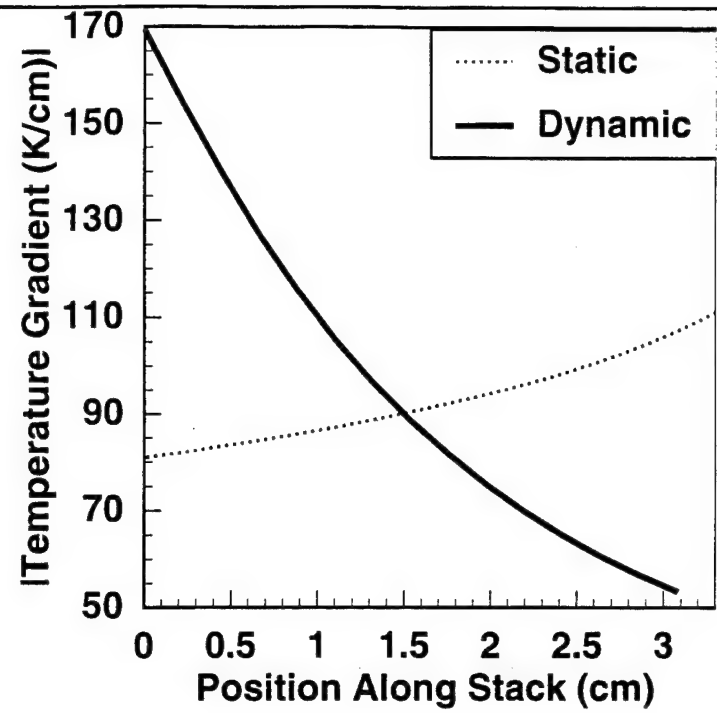

Figure 10. Prime mover stack static and dynamic temperature gradients.

Thermoacoustic power generation in the stack is proportional to the gradient of temperature. Figure 10 shows that static and dynamic temperature gradients are quite different. The hottest end of the prime mover stack (see Fig. 8 for the temperature scale) has more than 3 times the temperature gradient of the cold end, indicating (all other things being equal), that thermoacoustic power generation in the stack is greatest at the hot end.

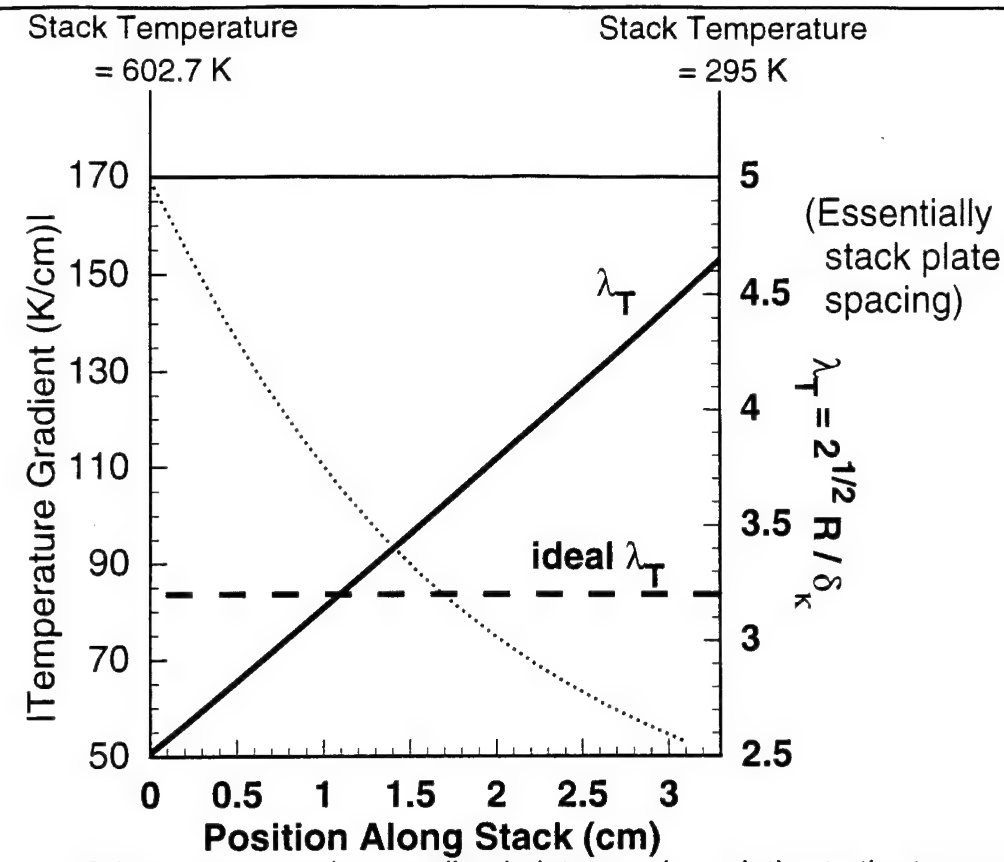

Figure 11. Prime mover stack normalized plate spacing relative to the temperature gradient and ideal inviscid thermoacoustics plate spacing.

Referring to the discussion below Fig. 10, all other things are not equal. Part of the reason the stack can achieve such a temperature gradient profile is due to the stack plate spacing. Figure 11 shows a composite of stack plate spacing and temperature gradient. Common sense short stack approximations discussed in Refs. 2 and 3 imply that the ideal plate spacing should be the value shown in Fig. 11, and that narrower plate spacing should be avoided. Optimization results seem to imply that the dynamical stack temperature gradient can be considerably increased by narrowing the stack, and that this narrowing is traded off against lower stack effectiveness. The stack location is in a region of low kinetic energy dissipation by gas viscosity, and the stack location also affects the dynamical temperature distribution.

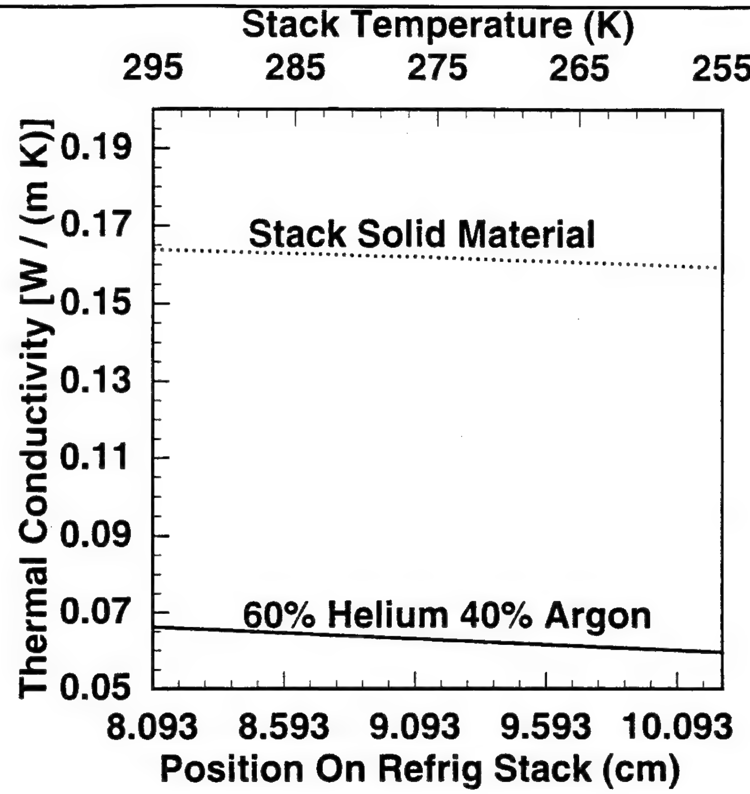

Figure 12. Refrigerator stack and gas thermal conductivities.

The refrigerator stack will now be considered in detail. Figure 12 shows the thermal conductivity of the stack solid and gas. The temperature span across the radial refrig stack is less severe than the plane-wave prime-mover stack. The refrig stack is also about 2/3 the length of the prime mover stack. The critical temperature separating prime mover and refrigerator operation is considerably higher for the radial refrig than the plane wave equivalent. This allows for use of a shorter radial stack for refrigeration than would be used in a plane wave refrig. The actual coordinates in the radial resonator are given for the refrig stack. Keep in mind that thermoacoustic refrigeration is proportional to the resonator cross sectional area, which of course increases with radius. The radial refrig stack location is a compromise between having the stack at a small radius to prevent kinetic energy dissipation by gas viscosity, and the other extreme of having the stack at a large radius to increase cooling capacity.

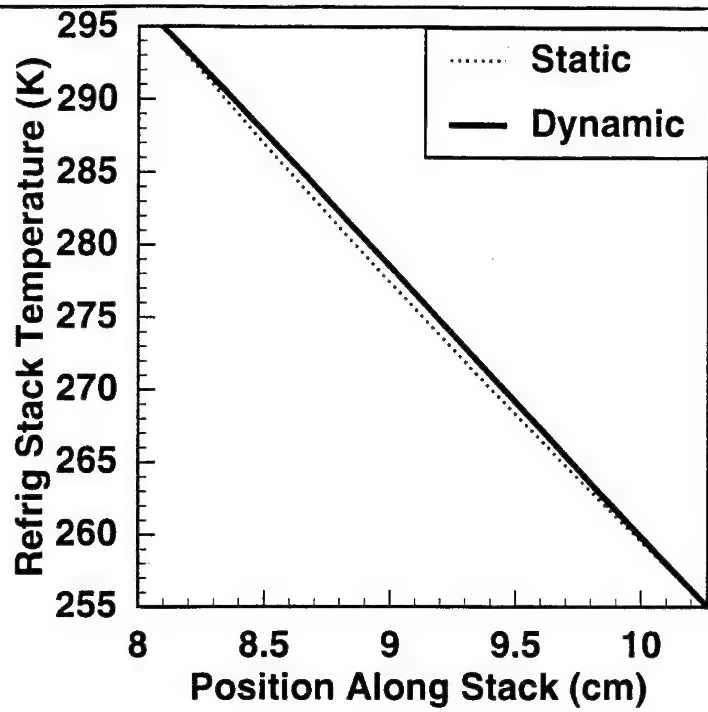

Figure 13. Refrigerator stack temperature distribution.

Figure 13 shows the refrigerator stack dynamical temperature distribution is similar to the static value.

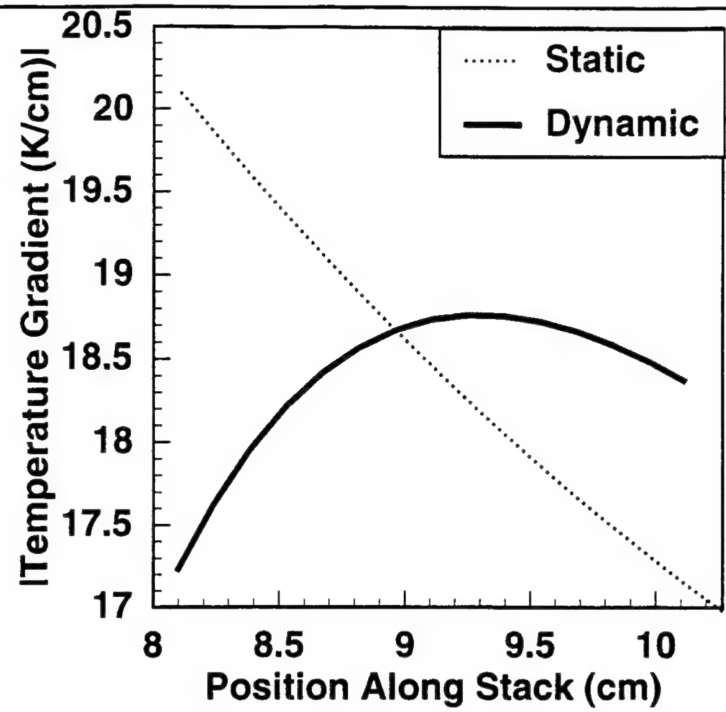

Figure 14. Refrigerator stack temperature gradient distribution.

Figure 14 shows the radial stack temperature gradient. The short stack approximation indicates that acoustic refrigeration is greatest with no temperature gradient. The stack location and plate spacing somewhat diminish the dynamical gradient, though the effect is not pronounced.

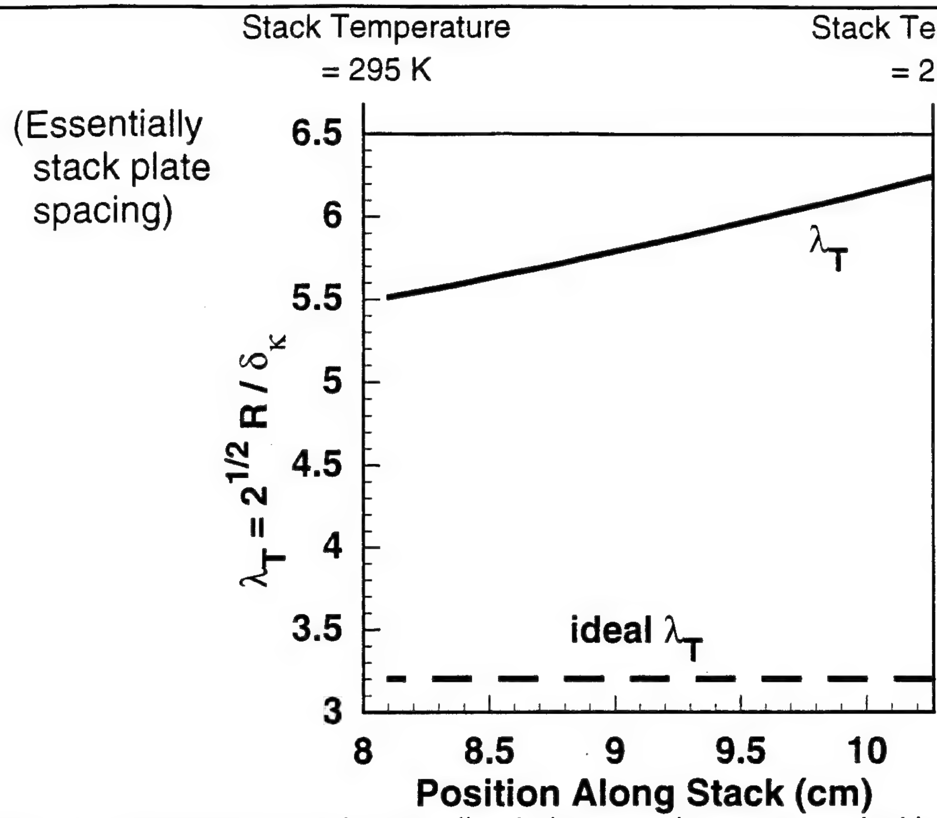

Figure 15. Refrigerator stack normalized plate spacing compared with the optimal plate spacing of ideal inviscid thermoacoustics.

Figure 15 shows that the normalized stack plate spacing for the refrig is considerably greater than the ideal inviscid gas plate spacing suggested by the short stack approximation. A similar result was observed in the refrig optimization based on the short stack approximation.[2] The radial refrig stack must be shoved out into the resonator far enough that appreciable heat is pumped (the resonator cross sectional area effect). Kinetic energy dissipation by gas viscosity increases as the stack is moved out, though is partially reduced by increasing the stack plate spacing as is evident in Fig. 15.

The biggest change in my intuition for thermoacoustics was the prime mover tradeoffs of plate spacing, location in the standing wave, and dynamical temperature gradient suggested by optimization.

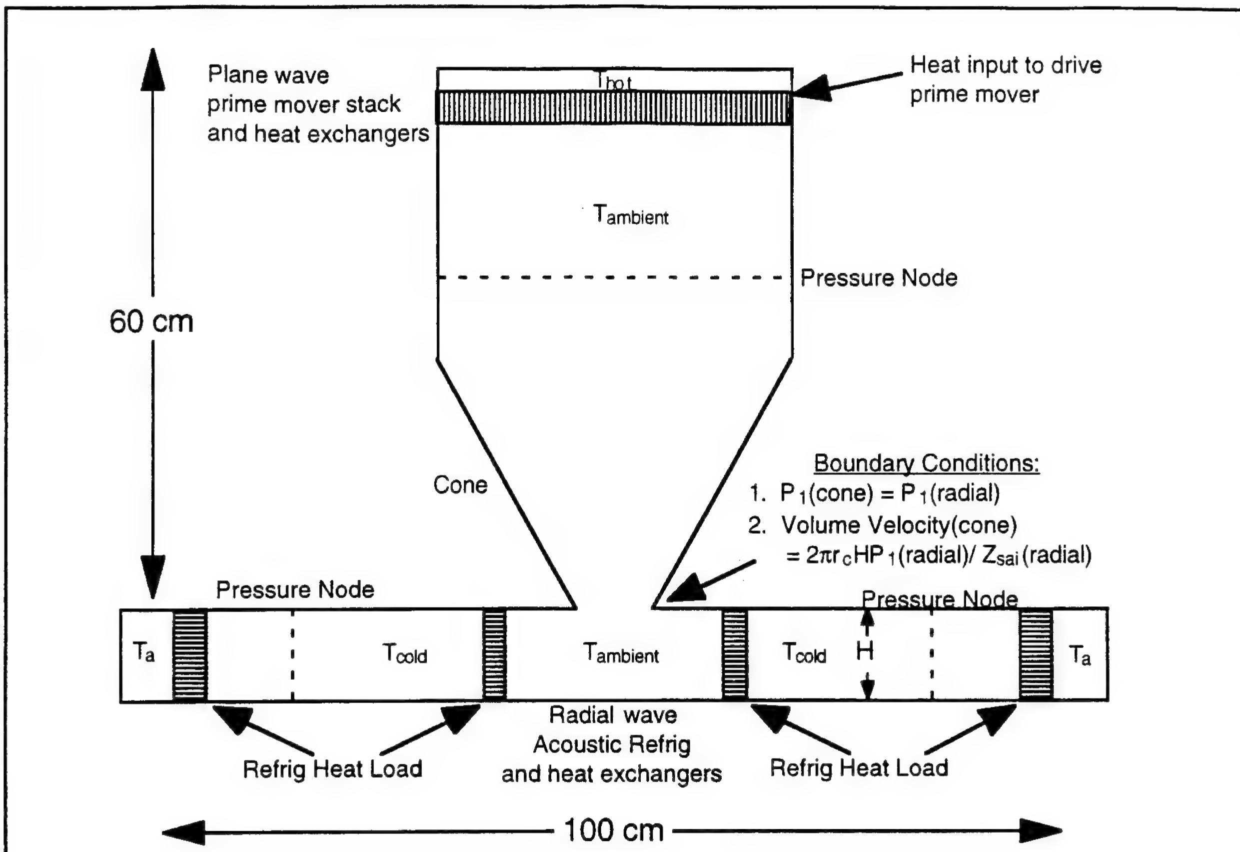

Figure 16. Heat-driven prime mover driving two radial wave acoustic refrigerators.

Steve Garrett commented that one should consider building a radial refrig with two stacks. Figure 16 shows such an arrangement. The extra radial refrig stack can be evaluated by adjusting the refrig heat load to match the cold end temperature boundary condition. The total refrig cooling capacity will be the sum of the radial inner and outer stacks. The refrig stack near the resonator wall is very similar to a plane wave refrig because curvature effects are less important at large radius.[2] The radial resonator is a large heat load for the refrig in Fig. 1, but not for the refrig in Fig. 16.

The heat driven refrig in Fig. 16 is an appropriate size for solar power to provide the heat input. The California and Nevada sun is most unbearable at the same time of year refrigeration and air conditioning are most in demand. Perhaps this is a niche for the acoustic refrig.

3b. Experiment *Jay Lightfoot, a Ph.D. student at the University of Mississippi, has succeeded in getting a radial wave prime mover to operate!* The goals of this experiment are to validate the numerical model, and to investigate the structure of harmonics that develop at high amplitude. Since resonator modes are not even close to being the same frequency as most harmonics, it is expected that this geometry will result in more energy in the fundamental than equivalent plane wave resonators. Our contribution to this work was in design and construction of heat exchangers, and in code development for system design. Jay is using silicon bonded mica paper stack material which has a thermal conductivity of 0.17 W/(m K) at room temperature, compared to 0.2 W/(m K) for Kapton, another material frequently used in stack construction. Parallel plates in the stack are concentric with the resonator axis. Heat exchangers are copper strips that are parallel to the resonator axis and perpendicular to the stack plates. A key finding of Jay's work is that the prime mover onset temperature was within 3 K of the predicted value. Work is currently underway to evaluate the spectral response at high amplitude.

4. References

1. G. W. Swift, "Thermoacoustic engines," J. Acoust. Soc. Am. **84**, 1145-1180 (1988).
2. W. P. Arnott, J. A. Lightfoot, R. Raspet, and H. Moosmüller, "Radial wave thermoacoustic engines: Theory and examples for refrigerators, prime movers, and high-gain narrow-bandwidth photoacoustic spectrometers," J. Acoust. Soc. Am. **99**, 734-745 (1996).
3. W. P. Arnott, H. E. Bass, and R. Raspet, "General formulation of thermoacoustics for stacks having arbitrarily shaped pore cross sections," J. Acoust. Soc. Am. **90**, 3228-3237 (1991).

OFFICE OF NAVAL RESEARCH
PUBLICATIONS/PATENTS/PRESENTATIONS/HONORS REPORT
for
01 June 95 through 31 May 96

Contract/Grant Number: N00014-93-1-1131

Principal Investigator: W. Patrick Arnott
Mailing Address with ZIP+4 if applicable: DESERT RESEARCH INSTITUTE
ATMOSPHERIC SCIENCES CENTER
PO BOX 60220
RENO NV 89506-0220

Phone Number: (702)-677-3123
Facsimile Number: (702)-677-3157
E-mail Address: pat@sage.dri.edu

a. Number of papers submitted to refereed journals but not yet published: 2

b. Number of papers published in refereed journals (ATTACH LIST): 2

c. Number of books or chapters submitted but not yet published: 0

d. Number of books or chapters published (ATTACH LIST): 0

e. Number of printed technical reports & non-refereed papers (ATTACH LIST): 0

f. Number of patents filed: 0

g. Number of patents granted (ATTACH LIST): 0

h. Number of invited presentations at workshops or professional society meetings: 1

i. Number of contributed presentations at workshops or professional society meetings: 1

j. Honors/awards/prizes for contract/grant employees, such as scientific society and faculty awards/offices (ATTACH LIST): 0

k. Number of graduate students supported at least 25% this year this contract/grant: 0

l. Number of post docs supported at least 25% this year this contract/grant: 0

How many of each are females or minorities? These six numbers are for ONR's EEO/Minority Reports. Minorities include Blacks, Aleuts, Amindians, etc., and those of Hispanic or Asian extraction/nationality. The Asians are singled out to facilitate meeting reporting semantics re "underrepresented".

Graduate student FEMALE: 0	Graduate student FEMALE: 0
Graduate student MINORITY: 0	Graduate student MINORITY: 0
Graduate student ASIAN E/N: 0	Graduate student ASIAN E/N: 0

LIST OF PUBLISHED PAPERS

1. W. P. Arnott, J. A. Lightfoot, R. Raspet, and H. Moosmüller, "Radial wave thermoacoustic engines: Theory and examples for refrigerators, prime movers, and high-gain narrow-bandwidth photoacoustic spectrometers," J. Acoust. Soc. Am. **99**, 734-745 (1996).
2. W. P. Arnott, H. Moosmüller, R. Abbott and M. D. Ossofsky, "Thermoacoustic enhancement of photoacoustic spectroscopy: Theory and measurements of the signal to noise ratio," Rev. Sci. Instrum. **66**, 4827-4833.

DISTRIBUTION LIST

2 COPIES
DR. LOGAN E. HARGROVE ONR 331
OFFICE OF NAVAL RESEARCH
800 NORTH QUINCY STREET
ARLINGTON VA 22217-5660

2 COPIES
DEFENSE TECHNICAL INFORMATION CENTER
8725 JOHN J. KINGMAN ROAD
FT. BELVOIR VA 22060-6218

FORM 298
ADMINISTRATIVE GRANTS OFFICER
OFFICE OF NAVAL RESEARCH
RESIDENT REPRESENTATIVE N00014
ADMINISTRATIVE CONTRACTING
OFFICER
1107 N.E. 45 ST.
SUITE 350
SEATTLE WA 98105-4631

DIRECTOR NAVAL RESEARCH LABORATORY
ATTN CODE 2667
4555 OVERLOOK AVENUE S.W.
WASHINGTON DC 20375-5326

NAVAL POSTGRADUATE SCHOOL
TECHNICAL LIBRARY CODE 0212
MONTEREY CA 93943

PROFESSOR ANTHONY A ATCHLEY
DEPARTMENT OF PHYSICS
CODE PH/AY
NAVAL POSTGRADUATE SCHOOL
MONTEREY CA 94943-5000

PROFESSOR HENRY E BASS
DEPARTMENT OF PHYSICS AND
ASTRONOMY
UNIVERSITY OF MISSISSIPPI
UNIVERSITY MS 38677

PROFESSOR STEVEN L. GARRETT
GRADUATE PROGRAM IN ACOUSTICS
PENNSYLVANIA STATE UNIVERSITY
P.O. BOX 30
STATE COLLEGE PA 16804

DR. KEITH A. GILLIS
THERMOPHYSICS DIVISION
NATIONAL INSTITUTE OF STANDARDS
AND TECHNOLOGY
GAITHERSBURG MD 20899-0001

PROFESSOR THOMAS J. HOFLER
DEPARTMENT OF PHYSICS
CODE PH/HF
NAVAL POSTGRADUATE SCHOOL
MONTEREY CA 93943-5000

PROFESSOR PHILIP L. MARSTON
DEPARTMENT OF PHYSICS
WASHINGTON STATE UNIVERSITY
PULLMAN WA 99164-2814

PROFESSOR ANDREA PROSPERETTI
DEPARTMENT OF MECHANICAL
ENGINEERING
JOHNS HOPKINS UNIVERSITY
BALTIMORE MD 21218

PROFESSOR RICHARD RASPET
DEPARTMENT OF PHYSICS AND
ASTRONOMY
UNIVERSITY OF MISSISSIPPI
UNIVERSITY MS 38677

PROFESSOR OREST G. SYMKO
DEPARTMENT OF PHYSICS
UNIVERSITY OF UTAH
SALT LAKE CITY UT 84112

DR. GREG SWIFT
LOS ALAMOS NATIONAL LAB
MS K764
LOS ALAMOS NM 87545

PROFESSOR MOISES LEVY
DEPARTMENT OF PHYSICS
UNIVERSITY OF WISCONSIN MILWAUKEE
MILWAUKEE WI 53201

PROFESSOR JULIAN D MAYNARD
DEPARTMENT OF PHYSICS
PENNSYLVANIA STATE UNIVERSITY
UNIVERSITY PARK PA 16802